Title

Assessment of shallow aquifer remediation capacity under different groundwater management conditions in CGS field

Journal

Arabian Journal of Geosciences, 9(6)

ISSN

1866-7511

Authors

Du, Shanghai

Zheng, Liange

Zhang, Wenjing

Publication Date

2016-05-01

DOI

10.1007/s12517-016-2479-6

Peer reviewed

Arab J Geosci (2016) 9: 448
DOI 10.1007/s12517-016-2479-6

Assessment of shallow aquifer remediation capacity under different groundwater management conditions in CGS field

Shanghai Du[1,2,3] & Liange Zheng [3] & Wenjing Zhang[1,2]

spaceAbstract Because of unknown faults and fractures in the overlying rock, CO_2 stored deep underground may move up- ward, and the intrusion may impact shallow groundwater quality. After leakage of CO_2 has ceased, the affected aquifer may show remediation capacity under natural conditions and injections and extractions. In this study, the reactive transport modeling software TOUGHREACT was used to simulate the remediation capacity of a study aquifer. The simulation results show that the intrusion of leaked CO_2 would decrease the pH of the target aquifer and trigger the dissolution of calcite min- erals. After CO_2 leakage has ceased, the pH would increase as would the concentration of Ca because of the dissolution of calcite along the flow path. Scenario simulation results of amelioration of groundwater quality by water injection and extraction show that single injection is the best option and a combination approach of injection and extraction could

spacecontrol the range of the affected area. The pH value should not be regarded as the single indicator for remediation capac- ity assessment. Parameter sensitive analysis results show that the rates of injection and extraction affect the repair results significantly.

Keywords Carbon dioxide leakage · Groundwater · Remediation · Calcite

Introduction

Carbon Dioxide Geological Storage (CGS) is one of the most effective methods of reducing the anthropogenic emissions of CO_2 and mitigating global climate change (Bachu 2000; Su et al. 2013; Du et al. 2015; Zhao et al.

2015). Because of the unknown faults and fractures in overlying rock, deep-stored CO_2 may move upward, and space
the intrusion impacts shallow groundwater quality space

Wenjing Zhang
zhangwenjing80@hotmail.com

[1] Key Laboratory of Groundwater Resources and Environment, Ministry of Education, Jilin University, Changchun 130021, China

[2] Institute of Water Resources and Environment, Jilin University, Changchun, China

[3] Earth Science Division, Lawrence Berkeley National Laboratory, Berkeley, USA

space(Smyth et al. 2009; Siirila et al. 2012; Yang et al. 2015; Zheng et al. 2015).

According to the published research, leaked CO_2 could decrease the pH of shallow groundwater, changing the controlling conditions of mineral dissolution/precipitation and adsorption/desorption, and thereby affecting the transport and transformation of metal species and organic matter in groundwater, and enhancing the risk of groundwater pollution (Zheng et al. 2009;

space

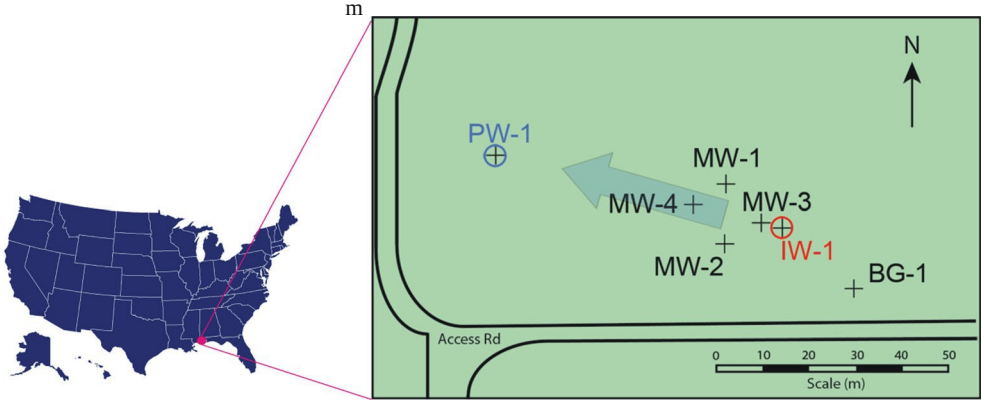

Fig. 1 Field test area and well location (*IW* injection well, *PW* pumping monitoring well, *BG* background

ound monitoring well)

space Lemieux 2011; Vong et al. 2011; Zhu et al. 2015). However, current research focusing on numerical simulation of the potential risks predominantly assume the presence of soluble minerals containing toxic metals

Table 1 Hydrogeology parameters used in the models

Parameters	Values
Porosity	0.3
Permeability (m^2)	1.44×10^{-11}
Compressibility coefficient (Pa^{-1})	2.8×10^{-9}
Diffusion coefficient (m^2/s)	1×10^{-9}
Dispersivity (m)	0.25
Tortuosity	0.67

space(such as PbS and FeS_2), and that the dissolution of these minerals could increase the concentration of these metals in groundwater (Humez et al. 2011; Vong et al. 2011). While complexation of Pb and As species are considered in these studies (Zheng et al. 2009) and they could provide preliminary conclusions for CO_2 leakage risk assessment, they do not provide an comprehensive assessment of the impact of leaked CO_2 on a potable aquifer. A comprehensive study requires site-scale studies, and a universal mechanism of response should be given more attention.

The results of indoor experiments show that when fluid containing CO_2 flows through columns containing potable aquifer media, the concentration of alkali and alkaline earth metal species increases, but concentrations of Pb and As do not increase significantly (Little and space

Table 2 Kinetic rate parameters for the reservoir

or

the

mineralls

dissolution/precipita

tion

Mineralls

A

(cm^2/g)

Parameters

fo

r

k

i

n

e

t

i

c

r

a

t

e

l

a

w

space

Table 3 Exchange coefficient for different ions to Na^+

Ions	Exchange coefficient($K_{Na\text{-}I}$)	Ions	Exchange coefficient($K_{Na\text{-}I}$)
K^+	0.2 (0.15∼0.25)	Ca^{2+}	0.40 (0.3∼0.6)
Mg^{2+}	0.50 (0.4∼0.6)	Sr^{2+}	0.35 (0.3∼0.6)

space

2010; Trautz et al. 2012; Zheng et al. 2012; Zheng et al. 2015). The lack of toxic metals (such as Pb and As) and minerals in potable aquifer media indicates that spacethe universal mechanism should be carbonate dissolution/ precipitation and ion exchange.

Compared with deep aquifers used for CGS, shallow aquifers experience greater recharge, allowing for self-remediation. The halting of CO_2 leakage could be caused by several factors: the lack of continuous CO_2 resources, a recharge of fresh groundwater would decrease the concentration of chemical species induced by CO_2 leakage, and mineral re-precipitation and re-adsorption would remediate the groundwater quality (Vong et al. 2011). Because of variable mineralogy and the kinetic rate of dissolution/precipitation and adsorption, aquifers exhibit variable self-remediation capacities. A numerical simulation could predict the variations in concentration of chemical species in groundwater and facilitate a more comprehensive assessment of CO_2 leakage risks and impacts on shallow groundwater quality (Esposito and Benson 2011).

space

Jackson 2010; Lu et al. 2010). Site-scale field tests indicate that mineral dissolution and ion exchange may be the controlling mechanisms behind the elevated CO_2 impacts on shallow groundwater quality (Kharaka et al.

Table 4 Species concentration of groundwater and injected water

Species	Groundwater	Injected water	Species	Groundwater	Injected water
pH	7.91	4.98	Sr	1.18E−06	1.18E−06
Ca	7.33E−05	7.33E−05	Mg	5.36E−05	5.36E−05
K	9.02E−05	9.02E−05	Na	6.79E−03	6.79E−03

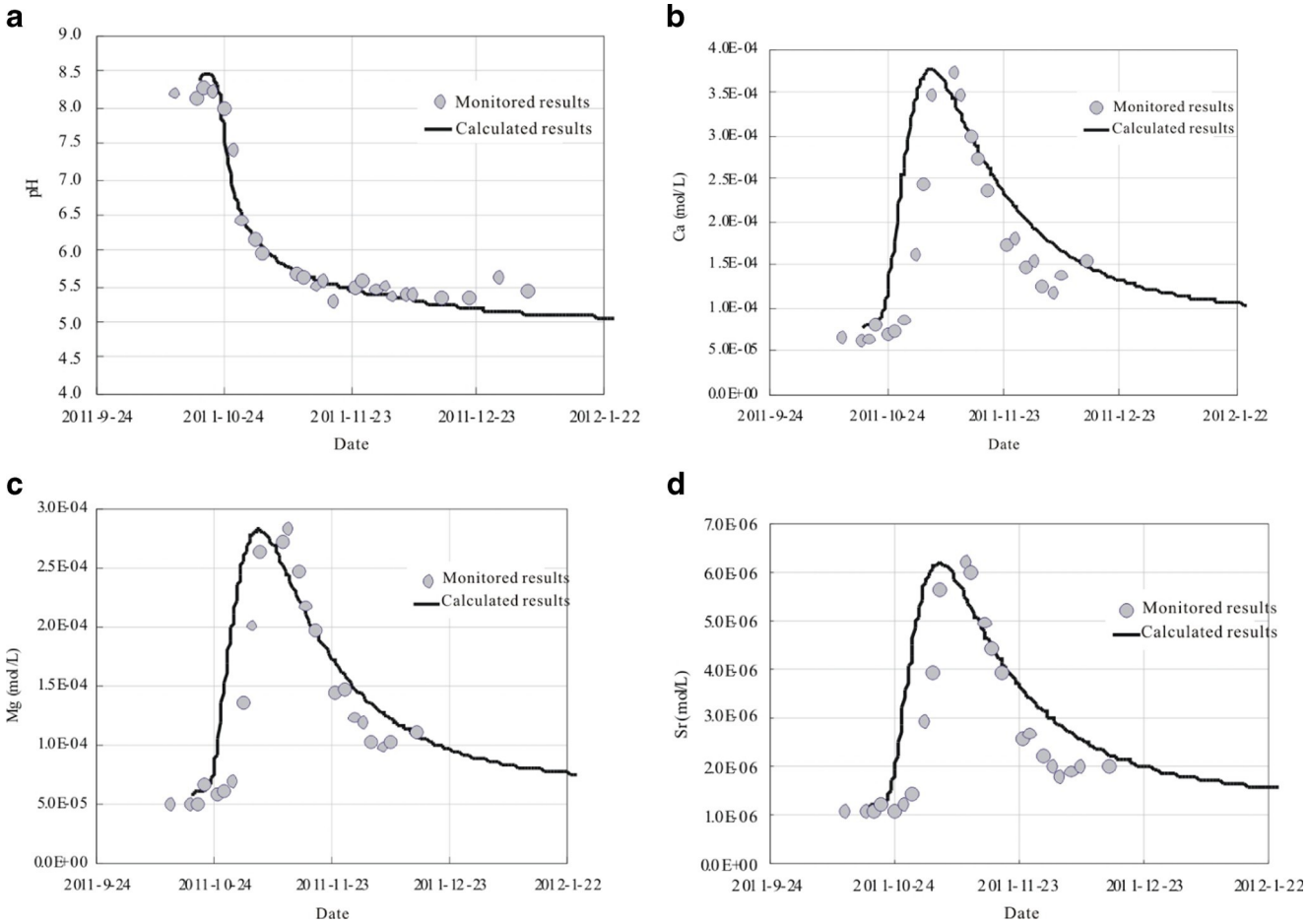

Fig. 2 Model fitting results of groundwater species at MW3 (data from Trautz et al. 2012): a pH, b Ca, c Mg, and d Sr

space

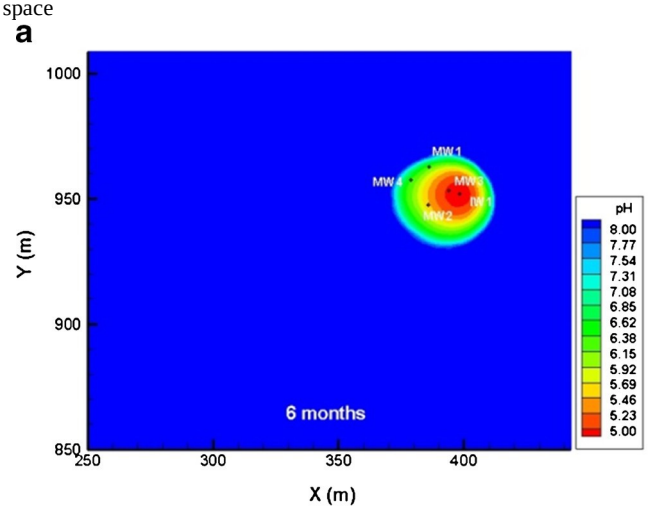

Fig. 3 Distribution of pH (a) and Ca (b) in groundwater after CO_2 leakage (6 months)

spaceField test results from the state of Mississippi, USA, were used in this study (Trautz et al. 2012; Zheng et al. 2015). This study examined the impacts of carbonate dissolution and ion exchange on the distribution of chemical species in groundwater, contrasting the remediation effects under different extraction-injection conditions after CO_2 leakage has ceased and assessing the impact of leaked CO_2 on groundwater quality for CGS projects.

Study area

The field test area is located near the town of Escatawpa, MS, USA, and the experiment was hosted

spaceby South Company Services at the Victor J. Daniel Electric Generating Plant (Trautz et al. 2012). The average precipitation in this area is 1876.4 mm/year and the average temperature of the Earth surface is ~18.89 °C.

According to field test requirements, seven wells were drilled in the field, as shown in Fig. 1. IW1 is a water injection well; PW1 is an extraction well; BG1 is a groundwater quality background monitoring well; and MW1, MW2, MW3, and MW4 are groundwater quality monitoring wells. The distance between IW1 and PW1 is 63.40 m and that between IW1 and MW3 is 4.63 m. The main hydrogeological variables of the target aquifer used in the model are shown in Table 1. The permeability of the target aquifer is 1.44×10^{-11} m^2, porosity

space

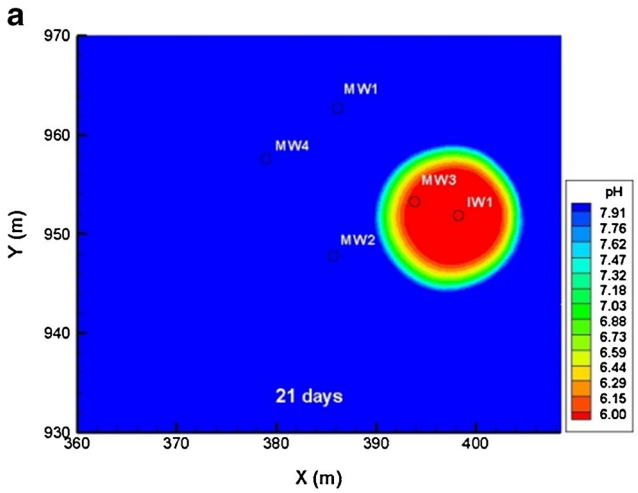

Fig. 4 Distribution of pH (a) and Ca (b) in groundwater after CO_2 leakage (21 days)

space

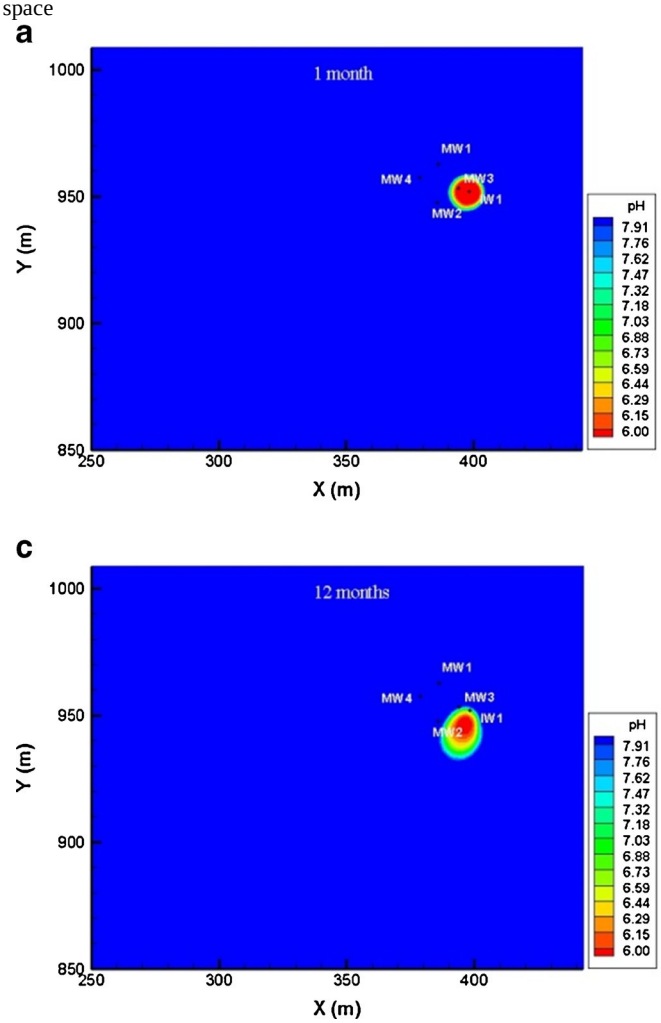

Fig. 5 Distribution of pH in groundwater after CO_2 leakage ceased (case 1) after a 1 month, b 6 months, c 12 months, and d 24 months

space

is 0.30, and a numerical dispersivity of ~0.25 m is used (Wu and Forsyth 2006; Trautz et al. 2012).

Methodology

Simulator

The multiphase flow and reactive transport simulator software TOUGHREACT (Xu et al. 2004) has been used in geothermal development and CO_2 geological storage and groundwater remediation (Smyth et al. 2009; Zheng et al. 2012; Kuo and Benson 2015), and version 2.0 of the software has been released with the additional capabilities of simulating biodegradation, adsorption/desorption of surface complexation, cation exchange, and coupled physicochemical reactions

space

(Apps et al. 2010; Xu et al. 2004; Xu et al. 2011; Salmasi and AZamathulla 2013; Zheng et al. 2009, 2012, 2015).

Geochemistry model

Although quartz, albite, K-feldspar, illite, and pyrite are the main minerals present within the target aquifer medium, carbonate was not detected. However, the pH-buffering capacity of the aquifer and the concentration variations of Ca, Mg, K, Na, and Sr in groundwater during the field test indicate that there may be carbonate minerals present of extremely low volume fractions (less than the detection limit of X-ray diffraction (XRD) and the total organic carbon-total inorganic carbon (TIC-TOC) test). The dissolution of a small quantity of carbonate could buffer the pH of groundwater during the

space

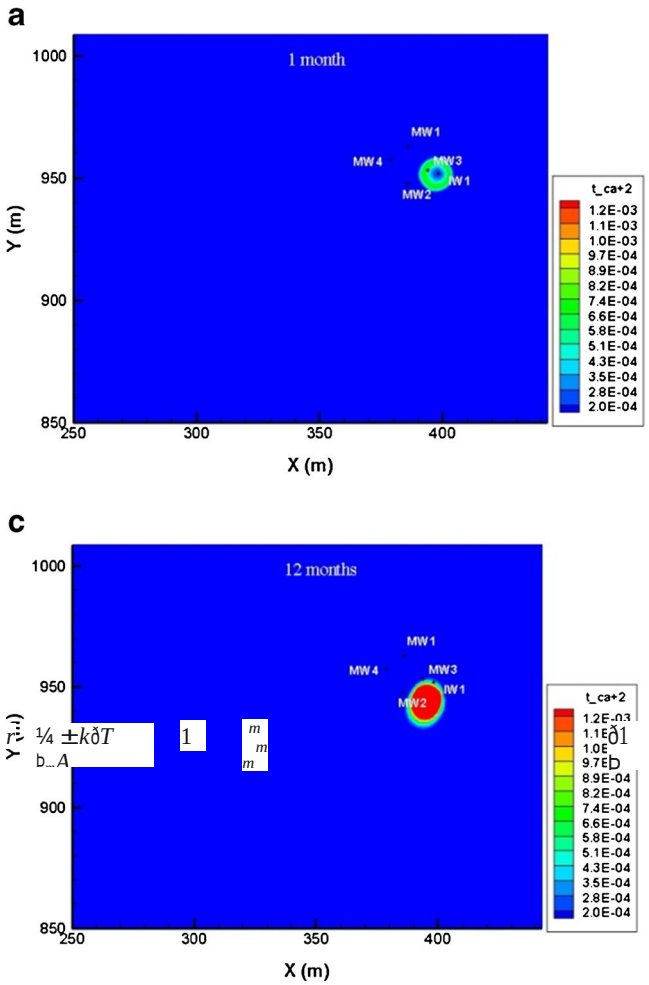

Fig. 6 Distribution of Ca in groundwater after CO2 leakage ceased (case 1) after a 1 month, b 6 months, c 12 months, and d 24 months

space field test, and the released Ca could drive cation exchange and alter the concentration of chemical species such as Ca, Mg, K, Na, and Sr in a similar way (Trautz et al. 2012). According to the simulation calibra- tion results, the initial volume fraction of calcite should be 0.175 % (which is lower than the detection limit of the XRD and TIC-TOC tests). The reactions to Fe-containing minerals were ignored in this study as the mechanism behind these reactions is not yet clear. The mechanisms behind dissolution of carbonate and cation exchange were considered.

The rates of mineral dissolution/precipitation could be impacted by temperature, pH, ion strength, and saturation conditions and can be expressed as (Lasaga et al. 1994; Steefel and Lasaga 1994):

space where r_m is the rate of dissolution/precipitation (positive indicates mineral dissolution and negative indicates pre- cipitation), $k(T_m)$ is the kinetic rate constant which is controlled by temperature (mol/L^{2}s), T is the environ- mental absolutely temperature (K), A_m is the specific surface area of a particular mineral (m^2/kg); K_m is the mineral equilibrium constant, Q_m is the ion activity prod- uct and, and θ and η are coefficients determined by ex- periment. If $Q_m = 0$, $r_m = k_m A_m$, and the mineral kinetic rate reaches the maximum value. As the mineral reaction proceeds, Q_m increases until Q_m equals K_m and r_m equals 0, and the reaction reaches its equilibrium state.

The kinetic rate constant of minerals $k(T)$ are the sum of three reaction mechanisms (Palandri and Kharaka 2004):

space

space

space

space

space

space

space

space

space

space

space

space where nu, H, and OH are the neutral, acid, and base mecha- nisms, respectively; E_a is the activation energy; k_{25} is the ki- netic rate constant at a temperature of 25 °C; R is the constant of air (J/mol K); and T is the environmental absolute temper- ature (K).

The minerals found in aquifer media of interest in this study are quartz (volume fraction of >60 % with a low kinetic rate constant) and calcite (volume frac- tion = 1.35×10^{-4}). The main chemical reaction between leaked CO_2 and minerals is

$$CO_2 + H_2O = H_2CO_3 \quad (3)$$

space other reactions are shown in Table 2 (Palandri and Kharaka 2004).

The reaction law of ion exchange is written as

$$nA^{m+} + mBX = mB^{n+} + nAX \quad (5)$$

where A^{m+} and B^{n+} are ions of A and B in solution, respec- tively, and AX and BX are the ions of A and B adsorbed on the solid, respectively. The exchange coefficient is expressed as

$\alpha^m y_A{}^n$

$_{space}CaCO_3$ þ H_2CO_3 ¼ $Ca^{2þ}$

$_{space}þ\ 2HCO_3^-$

spaceð4Þ

spaceK_{A-B} ¼

$_{space}B$

$\alpha^n y_B{}^m$

spaceð6Þ

space

spacewhere the kinetic rate constant = 5.0 × 10^{-6} mol/m^2 s and E_a = 23.5 kJ/mol. The kinetic rate constants of

spacewhere α_A and α_B is the activity of the chemical species in solution for the ions A and B, respectively, and y_A and y_B

space

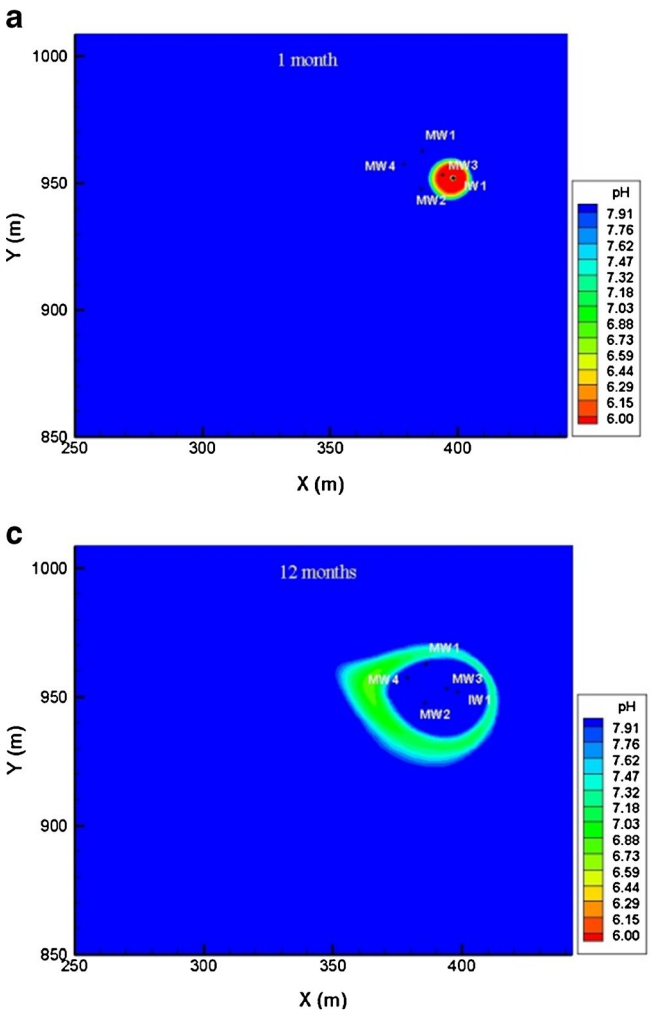

Fig. 7 Distribution of pH in groundwater after CO_2 leakage ceased (case 2) after a 1 month, b 6 months, c 12 months, and d 24 months

space

$_{space}$stand for the ion fraction absorbed onto the solid surface for the ions A and B, respectively. The exchange coefficients of ~~the ma~~in chemical species found in groundwater is shown in Table 3, and the exchange coefficients be- tween ions can be calculated using the data in this table (Appelo and Postma 2005; Zheng et al. 2012).

Results and discussions

Initial conditions and geochemical model validation

$_A$

According to the background quality monitoring results for groundwater, the background pH of the target aquifer is 7.96 and the initial concentration of Ca is 7.33 × 10^{-5} mol/L. There are two stages in the model:

space(1) to simulate CO_2 leakage, water saturated with CO_2 at a saturation pressure of 3.8 bars is injected into the target aquifer through IW1, and (2) to simulate the ceasing of CO_2 leakage, water with a background quality is injected into the target aquifer. The injection rate at IW1 is 8.2 m^3/day, the pumping rate of PW1 is 32.8 m^3/day, and the quality of the background groundwater and injected water is shown in Table 4.

The simulation started on November 18, 2011, and lasted for 180 days. The comparison between calculated concentrations and monitored results of pH, Ca, Mg, Sr, and K at MW3 are shown in Fig. 2. The calculated chemical species concentrations and monitoring results are in good agreement, which means that the dissolution of calcite and cation exchange aroused by Ca could explain the changes in chemical species concentration

space

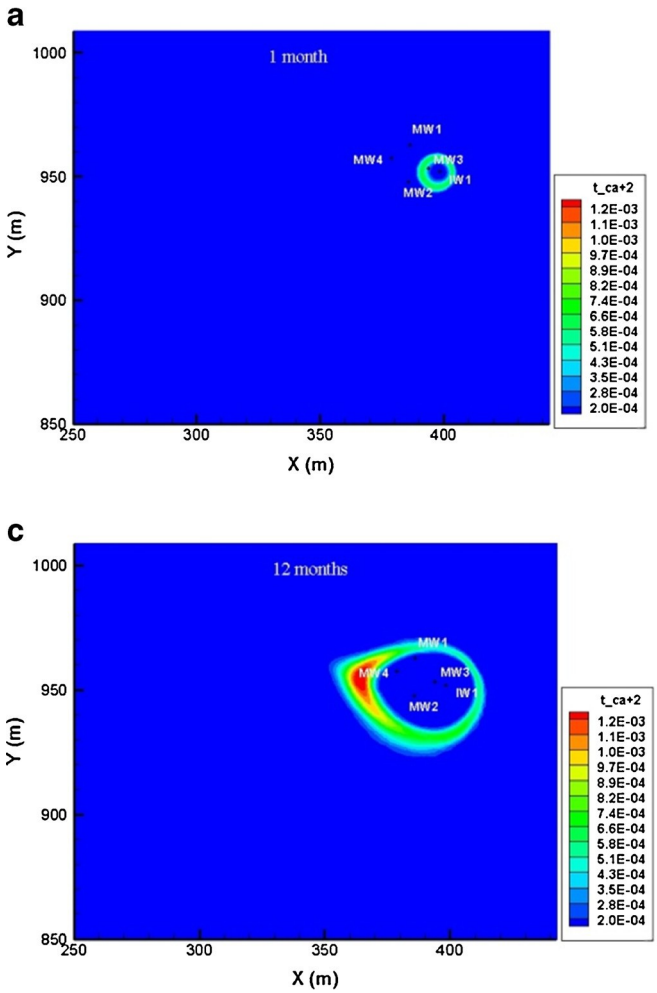

Fig. 8 Distribution of Ca in groundwater after CO_2 leakage ceased (case 2) after a 1 month, b 6 months, c 12 months, and d 24 months

space

spaceduring the field test and may be the controlling mechanisms during the test.

The discussions above indicate that injected CO_2 could impact the pH of groundwater and induce the dissolution of calcite and cation exchange. Therefore, the pH and concentration of Ca in groundwater should be comprehensively discussed in detail, as these two variables could reflect the groundwater quality changes during the field test, while the remediation effect can be discussed later.

Because of the injection of water at IW1 and the extraction at PW1, the distribution of pH and concentration of Ca in groundwater after the last 6 months after the leakage ceased as shown in Fig. 3. From the figures, it is evident that because of the injected water

spacebeing saturated with CO_2, pH decreased from an initial value of 7.96 to 4.98, a central-high plume formed, and the impact area extended with the continued leak- age. Because the concentration of H^+ increases when CO_2 is injected, calcite begins to dissolute and the concentration of Ca in groundwater begins to increase. As the volume of calcite is extremely low, the calcite dissolution completes rapidly, a donut-shaped plume is formed, and the impact area extends with the contin- ued leakage.

According to Fig. 2, the concentration of Ca in groundwater at MW3 would peak on the 21st day from the start of the test, and the distribution of chemical species in groundwater at this time (Fig. 4) has been set as the initial condition for the remediation prediction and assessment.

space

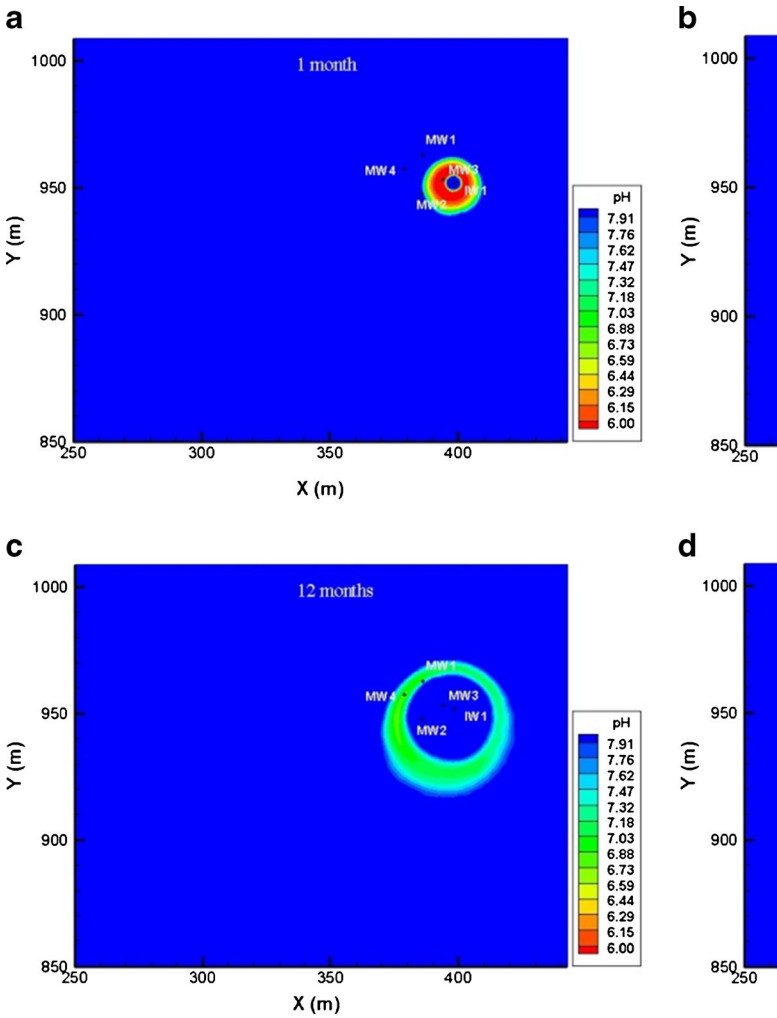

Fig. 9 Distribution of pH in groundwater after CO2 leakage ceased (case 3) after a 1 month, b 6 months, c 12 months, and d 24 months

space

spaceCase 1: natural conditions

Under natural conditions, no recharge or extraction occurs, and the transport of chemical species is driven by natural flow. The distribution changes of pH and concentration of Ca in groundwater under natural condi- tions is shown in Figs. 5 and 6, respectively. From Fig. 5, it is evident that the natural groundwater flows from the northeast to southwest (with a hydraulic gra- dient ~0.4 ‰). The impact plume extends slowly to the downstream of natural groundwater flow, and a significant oval plume is formed after 6 months.

During the formation of the oval plume, the impact area of high pH decreased because of the dilution of fresh groundwater and dissolution of calcite along the mitigation path.

From the distribution of changes of Ca in groundwater (Fig. 6), the donut-shaped plume is clearly seen, and spacethe increase in Ca concentration can be ascribed to the dissolution of calcite along the mitigation path. The concentration of Ca in groundwater increased from 4.77×10^{-4} mol/L at the beginning of the test to 5.21×10^{-3} mol/L (18 months later). Similar to the pH variations, an oval-shaped plume of Ca formed after 6 months moving downstream. The increase in high Ca impact area can be ascribed to the dissolution of calcite along the mitigation path.

Case 2: current extraction-injection conditions

The enhanced remediation methods refer to the methods of changing the initial flow field through injection and extraction, thereby accelerating the circulation rate of groundwater and reducing the concentration of pollutants. The injection method dilutes the concentration of pollutants, or specific substances are added to the space

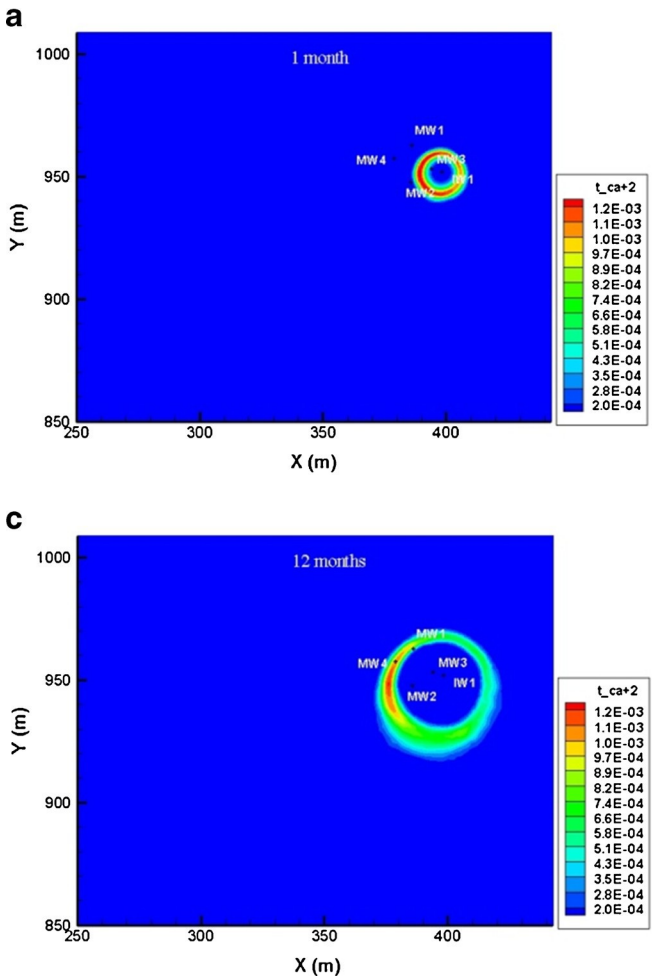

Fig. 10 Distribution of Ca in groundwater after CO2 leakage ceased (case 3) after a 1 month, b 6 months, c 12 months, and d 24 months

space

spaceinjected water to improve the efficiency of groundwater remediation. The extraction method pumps groundwater with a high concentration of pollutants up to the sur- face, which could efficiently reduce the concentration of pollutants in groundwater. However, the pumped water requires further purification treatment.

Current extraction-injection conditions are the injec- tion of water at IW1 at a rate of 8.2 m^3/day and the extraction of water at PW1 at a rate of 32.8 m^3/day. The injected water quality has been changed to water with the background quality of the target aquifer and the predicted groundwater quality variations after CO_2 leakage ceased. The variations in distribution of pH and Ca concentration in groundwater are shown in Figs. 7 and 8, respectively, and display similar transformations of the impact plume.

spaceFrom the variations in distribution of pH (Fig. 7), it can be seen that, because of the injection of high pH water at IW1, a donut-shaped plume is formed from the beginning. The total impacted area extends toward PW1 and can be ascribed to the local flow field formed by the injection of water at IW1 and extraction of water at PW1, causing the central part of plume with high pH to extend synchronously. During the mitigation of H^+ in groundwater, the injected water of background pH dilutes the impacted groundwater and the dissolution of calcite consumes H^+ in groundwater, resulting in an in- creasing trend of pH until the background value is obtained.

Although the plume transformation is similar between pH and Ca, the initial increase in Ca concentration in groundwater can be ascribed to the dissolution of

space

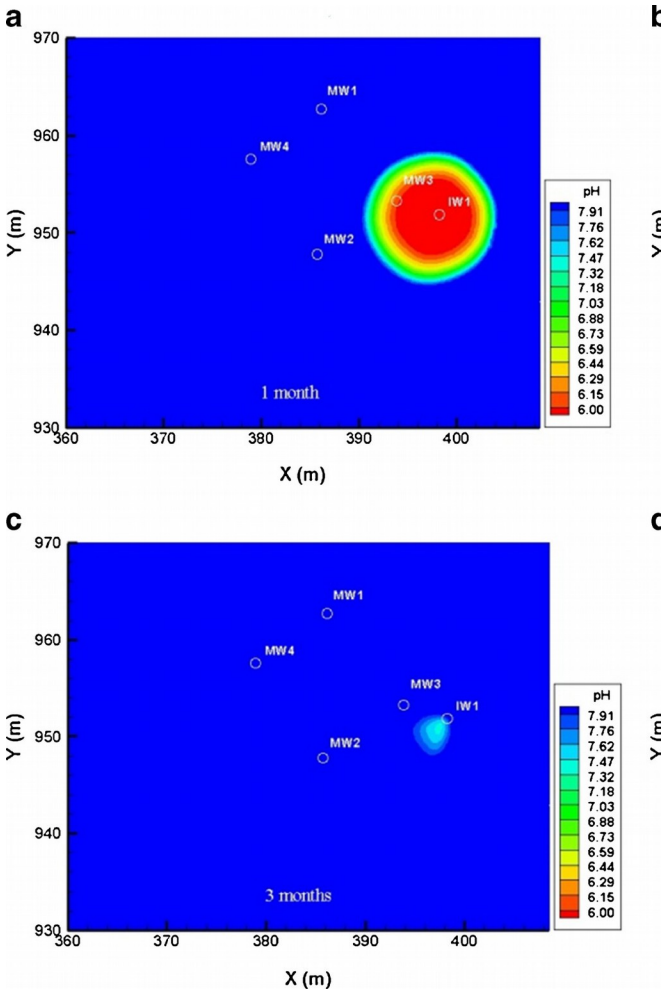

space

space calcite, and the subsequent decreased concentration can be ascribed to dilution because of fresh injected water. The original expansion of the donut-shaped plume of Ca in groundwater can be ascribed to the flow field. The dissolution of calcite at the new impact area would sig- nificantly increase the concentration of Ca in groundwa- ter. The concentration of Ca in groundwater increased from 4.76×10^{-4} mol/L at the beginning of the test to 1.74×10^{-3} mol/L after 6 months and then decreased to 5.16×10^{-4} mol/L at 24 months. The current conditions could extend the area of plume and enhance the concentration of Ca in groundwater.

Case 3: IW1 injection only

This is the injection of water at IW1 without extraction of water at PW1. The variations in distribution of pH and Ca spaceconcentration in groundwater are shown in Figs. 9 and 10, respectively. The distribution shape transformations of pH and Ca in groundwater are similar. Comparing the simu- lation results of cases 2 and 3 indicates that ceasing ex- traction of groundwater at PW1 results in the movement of the plumes of pH and Ca concentration in groundwater toward the downstream region of the natural flow field. Similar to case 2, the dilution of fresh groundwater and dissolution of calcite control the shape transformations and the distributions of the concentration of H^+ and Ca in groundwater. The concentration of Ca in groundwater increased from 4.76×10^{-4} to 1.78×10^{-3} mol/L after 6 months and then decreased to 6.56×10^{-4} mol/L after 24 months, values closely resembling those in case 2. Injection of water at IW1 could result in the extension of the plume area and an enhancement of the concentration of Ca in groundwater.

space

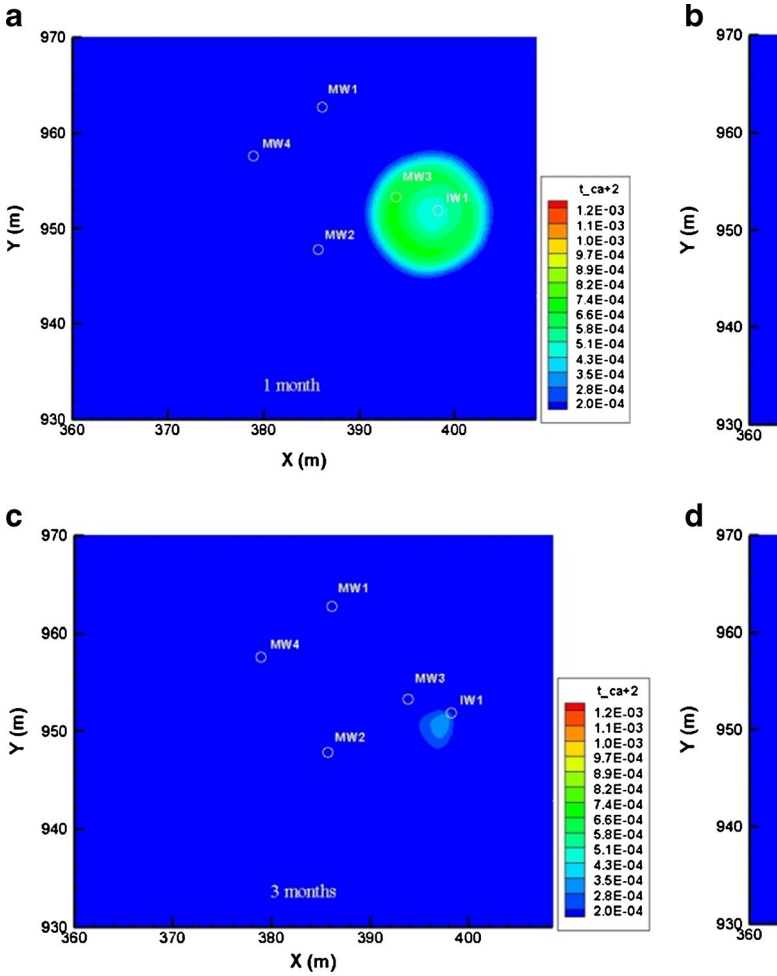

Fig. 12 Distribution of Ca in groundwater after CO_2 leakage ceased (case 4) after a 1 month, b 2 months, c 3 months, and d 4 months

space

space Case 4: IW1 extraction only

The case of IW1 extraction only was achieved by using IW1 as an extraction well at a rate 8.2 m^3/day and not utilizing PW1 as an extraction well. The distribution of pH and Ca concentration is shown in Figs. 11 and 12, respectively. From the figures, it is evident that the transformations of the impact plume are similar between pH and Ca. The area of the impact plume decreased rapidly after the extraction at IW1 and was almost in- distinguishable after 3 months. Although the concentra- tion of Ca in groundwater

increased around the extrac- tion well, the duration is too short and the area is too small to conclude that extraction at IW1 only could reduce and remove the impact plume significantly.

spaceCase 5: conditions of extraction at IW1 and injection at MW1, MW2, and MW4

To enhance the remediation efficiency based on case 4, additional injection wells (MW1, MW2, and MW4, with injection rate 8.2 m^3/day) have been used in case 5. The variations in the pH distributions and Ca concentrations in groundwater are shown in Figs. 13 and 14, respectively. From the figures, it is evident that the transformations of the impact plumes are similar between pH and Ca concentration in groundwater. Unfortunately, the new added injection results in a new flow field, forming a tail plume at the southeast side of IW1. The concen-
tration of Ca in groundwater reaches 1.14×10^{-3} mol/L from 4.77×10^{-4} mol/L at the beginning of the test.
space

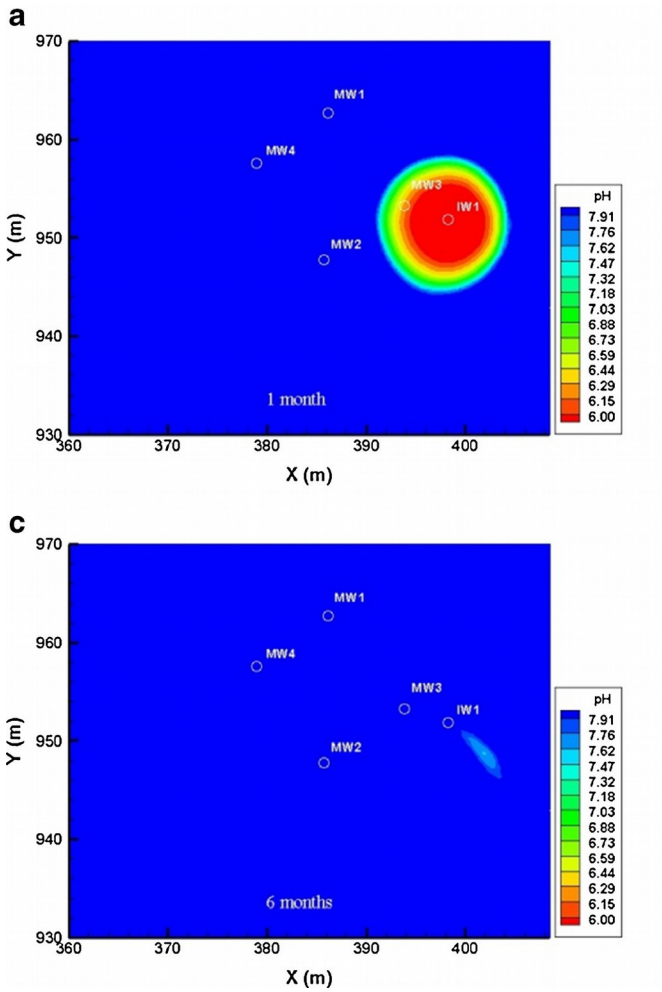

space

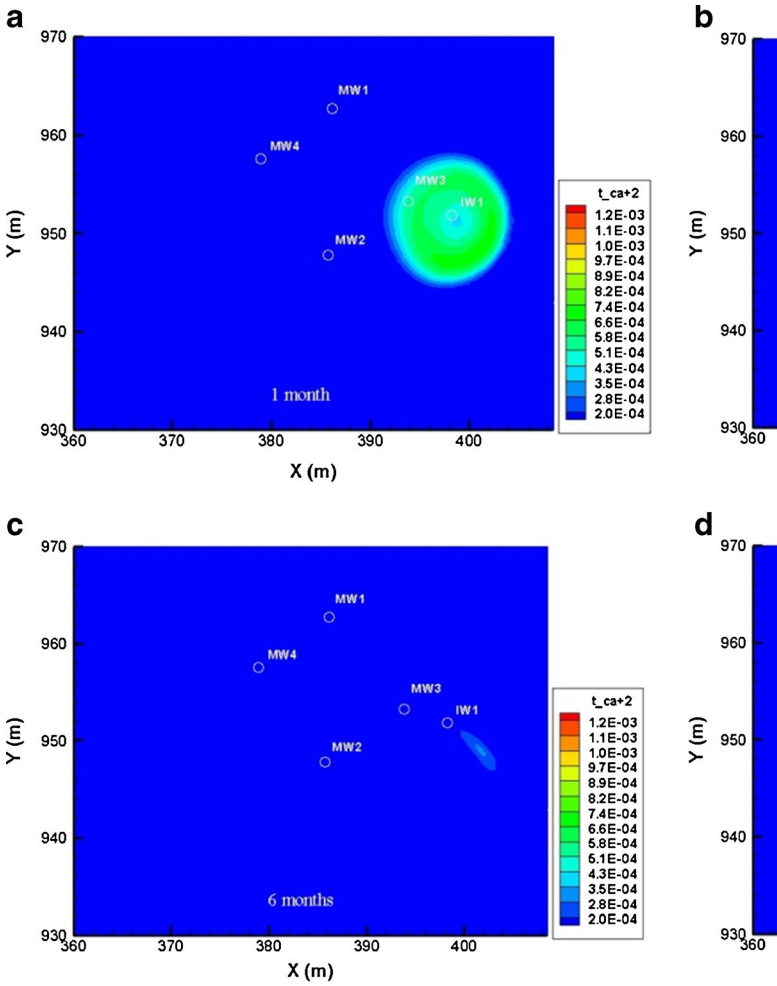

Fig. 14 Distribution of Ca in groundwater after CO_2 leakage ceased (case 5) after a 1 month, b 3 months, c 6 months, and d 9 months

space

The simulation results of case 5 indicate that the rate of injection/extraction significantly impacts the remediation efficiency.

Case 6: condition of injection at IW1 and extraction at MW1, MW2, and MW3

Case 6 is based on case 5 and all the injection/extraction properties of the wells changed; the injection rate at IW1 was changed to 8.2 m^3/day and the extraction rates at MW1, MW2, and MW3 were changed to 8.2 m^3/day. The variations in the pH distribution and Ca concentration in groundwater are shown in Figs. 15 and 16, respectively. From the figures it is evident that the transformations of impact plumes are similar between pH and Ca concentration in groundwater. The impact plumes moved toward the extraction wells, and the pH increased due to the dilution
space
by freshwater and buffering of calcite. The concentration of Ca in groundwater increased to 7.76×10^{-4} mol/L after 3 months and then decreased to 7.98×10^{-5} mol/L after 24 months. Although the impact area could be controlled

in this case, the concentration of Ca in groundwater increased significantly during the remediation.

Sensitivity analysis of extraction rates

The rates of injection/extraction could impact the remediation efficiencies. A sensitivity analysis of extraction rates has been performed based on case 4. The extraction rates at IW1 were set as 0.37852, 0.18926, 0.09463, 0.04732, and 0.02366 kg/s, and the pH variations and Ca concentrations in the groundwater at MW3 are shown in Fig. 17. From the figure, we can see that pH almost reaches its background value under different

space

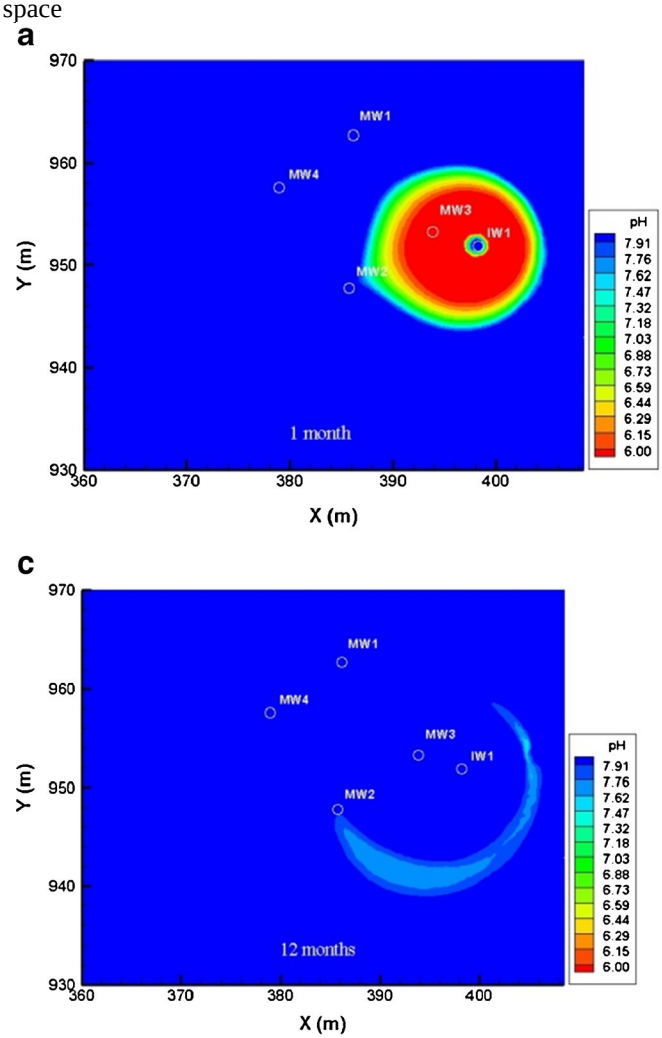

Fig. 15 Distribution of pH in groundwater after CO_2 leakage ceased (case 6) after a 1 month, b 6 months, c 12 months, and d 18 months

space

extraction rates, but the elevating rates of pH values increase with increasing groundwater extraction rates. However, the peak concentrations of Ca in groundwater decrease with increasing groundwater extraction rates, which means that the increasing extraction rate could enhance the remediation efficiency significantly.

Conclusions

1. Leakage of CO_2 impacts shallow groundwater quality through dissolution/precipitation and cation exchange of minerals. The dissolution of calcite and cation exchange explains the concentration changes for Ca, Mg, Sr, and K in groundwater.

space

2. After the leakage of CO_2 ceased under the natural and flow fields, the shallow aquifer exhibited variable reme- diation capacity, and extraction is the better choice to re- move impacts.
3. The concentration of Ca and H^+ exhibited different trends which can be ascribed to different impact mechanisms. The pH and concentration of other species should be considered during the remediation process.
4. The sensitivity analysis results indicate that the acidic pH values increased and the peak concentrations of Ca in groundwater decreased with increasing groundwater extraction rates. This means that an increasing rate of extraction could enhance the remediation efficiency significantly.

space

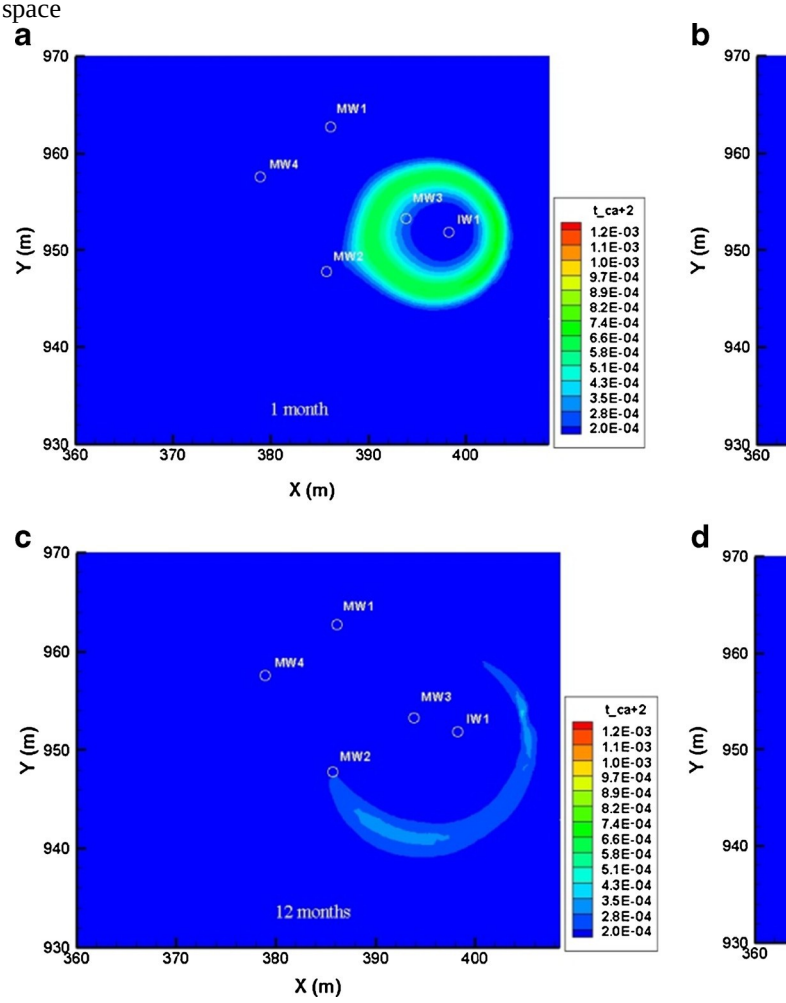

Fig. 16 Distribution of Ca in groundwater after CO_2 leakage ceased (case 6) after a 1 month, b 6 months, c 12 months, and d 18 months

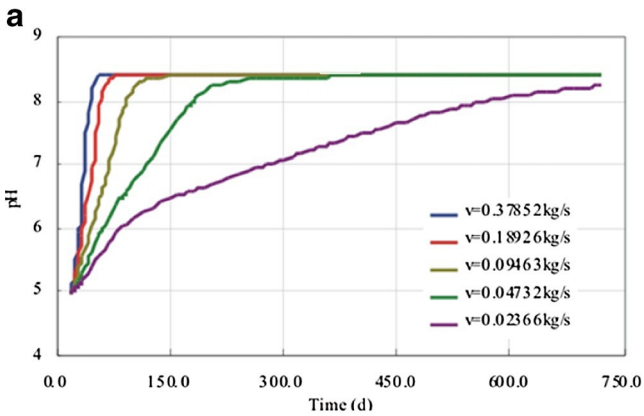

Fig. 17 Extraction rate sensitivities to pH (a) and Ca concentration (b) in groundwater

space

spaceAcknowledgments This work was supported by the Electric Power Research Institute; the EPA, Office of Water, under an Interagency Agreement with the US Department of Energy (DOE) at LBNL, under contract number DE-AC02-05CH11231; and the Assistant Secretary for Fossil Energy, National Energy Technology Laboratory (NETL), National Risk Assessment Program (NRAP), of the US Department of Energy under contract number DEAC02-05CH11231. This work also was supported by the Jilin Province Science and Technology Development Plan (No. 20140520143JH) and the Multi-Subjects Research Program for Ph.D. Student in Jilin University (2011J012). Thanks to the anonymous reviewers' and editor's suggestions and com- ments which greatly helped the authors to improve the quality of the paper.

References

Appelo CAJ, Postma D (2005) Geochemistry, groundwater and pollution.
A. A. Balkema, Rotterdam

Apps JA, Zheng L, Zhang Y (2010) Evaluation of groundwater quality changes in response to CO_2 leakage from deep geological storage. Transp Porous Media 82:215–246. doi:10.1007/s11242-009-9509-8

Bachu S (2000) Sequestration of CO_2 in geological media: criteria and approach for site selection in response to climate change. Energy Conserv Manag 42:953–970. doi:10.1016/S0196-8904(99)00149-1

Du SH, Su XS, Xu W (2015) Assessment of CO_2 geological storage capacity in oilfields of Songliao Basin, Northeastern China. Geosci J. doi:10.1007/s12303-015-0037-y

Esposito A, Benson SM (2011) Remediation of possible leakage from geologic CO_2 storage reservoirs into groundwater aquifers. Energy Procedia 4:3216–3223. doi:10.1016/j.egypro.2011.02.238

Humez P, Audigane P, Lions J (2011) Modeling of CO_2 leakage up through an abandoned well from deep saline aquifer to shallow fresh groundwater. Transport porous Meida 90:153–181. doi:10.1007/ s11242-011-9801-2

Kharaka YK, Thordsen JJ, Kakouros E (2010) Changes in the chemistry of shallow groundwater related to the 2008 injection of CO_2 at the ZERT field site, Bozeman, Montana. Environmental Earth Sciences 60:273–284. doi:10.1007/s12665-009-0401-1

Kuo CW, Benson SM (2015) Numerical and analytical study of effects of small scale heterogeneity on CO_2/brine multiphase flow system in horizontal corefloods. Adv Water Resour 79:1–17. doi:10.1016/j. advwatres.2015.01.012

Lasaga AC, Soler JM, Ganor J (1994) Chemical weathering rate laws and global geochemical cycles. Geochim Cosmochim Acta 58:2361– 2386. doi:10.1016/0016-7037(94)90016-7

Lemieux JM (2011) Review: the potential impact of underground geological storage of carbon dioxide in deep saline aquifer on shallow groundwater resources. Hydrogeol J 19:757–778. doi:10.1007/ s10040-011-0715-4

Little MG, Jackson RB (2010) Potential impacts of leakage from deep CO_2 geosequestration on overlying freshwater aquifers. Environmental Science & Technology 44:9225–9232. doi:10.1021/es102235w

Lu JM, Partin JW, Hovorka SD (2010) Potential risks to freshwater resources as a result of leakage from CO_2 geological storage: a batch- reaction experiment. Environ Earth Sci 60:335–348. doi:10.1007/ s12665-009-0382-0

Palandri JL and Kharaka YK (2004) A compilation of rate parameters of water-mineral interaction kinetics for application to geochemical modeling. U. S. Geological Survey report (2004-1068)

spaceSalmasi F, AZamathulla HM (2013) Determination of optimum relaxa- tion coefficient using finite difference method for groundwater flow. Arab J Geosci 6:3409–3415. doi:10.1007/s12517-012-0591-9

Siirila ER, Nacarre-sitchler AK, Maxwell RM, McCray JE (2012) A quantitative methodology to assess the risk to human health from CO_2 leakage into groundwater. Adv Water Resour 96:146–164. doi: 10.1016/j.advwatres.2010.11.005

Smyth RC, Hovorka SD, Lu J (2009) Assessing risk to fresh water resources from long term CO_2 injection- laboratory and field studies. Energy Procedia 1:1957–1964. doi:10.1016/j.egypro.2009.01.255

Steefel CI, Lasaga AC (1994) A coupled model for transport of multiple chemical species and kinetic precipitation/dissolution reactions with application to reactive flow in single phase hydrothermal systems. Am J Sci 294:529–592. doi:10.2475/ajs.294.5.529

Su XS, Xu W, Du SH (2013) Basin-scale storage capacity assessment of deep saline aquifers in the Songliao Basin, Northeastern China. Greenhouse Gases: Sci Technol 3:266–280. doi:10.1002/ghg.1354

Trautz RC, Pugh JD, Varadharajan C, Zheng L, Bianchi M, Nico PS, Spycher NF, Newell DL, Esposito RA, Wu Y, Dafflon B, Hubbard SS, Birkholzer JT (2012) Effect of dissolved CO_2 on a shallow groundwater system—a controlled release field experiment. Environ Sci Technol 47:298–305. doi:10.1021/es301280t

Vong CQ, Jacquemet N, Picot-Colbeaux G (2011) Reactive transport modeling for impact assessment of a CO_2 intrusion on trace elements mobility within fresh groundwater and its natural

		Neutral mechanism		Acid mechanism			Base mechanism		
		k_{25}	E_a	k_{25}	E_a	n (H^+)	k_{25}	E_a	n (H^+)
Cal Calcite	9.8	5.0×10^{-06}	23.5						
Qu Quartz	9.1	1.0×10^{-14}	87.7						
Kao Kaolinite	108.7	6.92×10^{-14}	22.2	4.90×10^{-12}	65.9	0.777	8.91×10^{-18}	17.9	−0.472
Illit Illite	108.7	1.66×10^{-13}	35.0	1.05×10^{-11}	23.6	0.34	3.02×10^{-17}	58.9	−0.40
K-f K-feldspar	9.1	3.89×10^{-13}	38.0	8.71×10^{-11}	51.7	0.5	6.31×10^{-22}	94.1	−0.823
Oli Oligoclase	9.1	1.44×10^{-12}	69.8	2.14×10^{-10}	65.0	0.457			
Alb Albite	9.1	2.75×10^{-13}	69.8	6.92×10^{-11}	65.0	0.457	2.51×10^{-16}	71.0	−0.572
Sec Secondary minerals									
Ma Magnesite	9.1	4.57×10^{-10}	23.5	4.17×10^{-07}	14.4	1.0			
Dol Dolomite	12.9	2.95×10^{-08}	52.2	6.46×10^{-04}	36.1	0.5			
Na-smectite	151.6	1.66×10^{-13}	35.0	1.05×10^{-11}	23.6	0.34	3.02×10^{-17}	58.9	−0.40

groundwater quality and monitoring-network efficiency: case study at a CO2 enhanced oil recovery site. Environ Sci Technol 49:8887–8898. doi:10.1021/acs.est.5b01574

Zhao RR, Cheng JM, Zhang K, Liu N, Xu FQ (2015) Numerical inves- tigation of basin-scale storage of CO2 in saline aquifers of Songliao Basin, China. Greenhouse Gases: Sci Technol 5:180–197. doi:10. 1002/ghg.1473

Zheng L, Apps JA, Zhang Y (2009) On mobilization of lead and arsenic in groundwater in response to CO_2 leakage from deep geological storage. Chem Geol 268:281–297. doi:10.1016/j.chemgeo.2009.09.007

Zheng L, Apps JA, Spycher N (2012) Geochemical modeling of changes in shallow groundwater chemistry observed during the MSU-ZERT CO_2 injection experiment. Int J Greenhouse Gas Control 7:202–217. doi:10.1016/j.ijggc.2011.10.003

Zheng L, Spycher N, Varadharajan C, Tinnacher RM, Pugh JD, Bianchi M, Birkholzer J, Nico PS, Trautz RC (2015) On the mobilization of metals by CO2 leakage into shallow aquifers: exploring release mechanisms by modeling filed and laboratory experiments. Greenhouse Gases: Sci Technol 5:403–418. doi:10.1002/ghg.1493

Zhu QL, Li XC, Jiang ZB, Wei N (2015) Impacts of CO2 leakage into shallow formations on groundwater chemistry. Fuel Process Technol 135:162–167. doi:10.1016/j.fuproc.2014.11.042

Table 2 Kinetic rate parameters for the minerals dissolution/p

Minerals	A (cm^2/g)	Parameters for kinetic rate la	
		Neutral mechanism	
		k_{25}	E_a
Calcite	9.8	5.0×10^{-06}	23.5
Quartz	9.1	1.0×10^{-14}	87.7
Kaolinite	108.7	6.92×10^{-14}	22.2
Illite	108.7	1.66×10^{-13}	35.0
K-feldspar	9.1	3.89×10^{-13}	38.0
Oligoclase	9.1	1.44×10^{-12}	69.8
Albite	9.1	2.75×10^{-13}	69.8
Secondary minerals			
Magnesite	9.1	4.57×10^{-10}	23.5
Dolomite	12.9	2.95×10^{-08}	52.2
Na-smectite	151.6	1.66×10^{-13}	35.0
Ca-smectite	108.7	1.66×10^{-13}	35.0

Steefel and Lasaga 1994):

$$r_m = \pm k(T)_m A_m \left[1 - \left(\frac{Q_m}{K_m{}^m}\right)^{\theta}\right]^{\eta}$$

Table 3 Exchange coefficient for different ions to N

Ions	Exchange coefficient(K_{Na-I})	Ions	Exchange
K^+	0.2 (0.15~0.25)	Ca^{2+}	0.40 (0.3~
Mg^{2+}	0.50 (0.4~0.6)	Sr^{2+}	0.35 (0.3~

Jackson 2010; Lu et al. 2010). Site-scale fi
cate that mineral dissolution and ion exch
the controlling mechanisms behind the elev
pacts on shallow groundwater quality (K

Table 4 Species concentration of groundwater and i

Species	Groundwater	Injected water	Species	Ground
pH	7.91	4.98	Sr	1.18E−(
Ca	7.33E−05	7.33E−05	Mg	5.36E−(
K	9.02E−05	9.02E−05	Na	6.79E−(

where nu, H, and OH are the neutral, acid, and base
nisms, respectively; E_a is the activation energy; k_{25} i
netic rate constant at a temperature of 25 °C; R is the
of air (J/mol K); and T is the environmental absolute
ature (K).

The minerals found in aquifer media of interes
study are quartz (volume fraction of >60 % wit
kinetic rate constant) and calcite (volum
tion = 1.35×10^{-4}). The main chemical reaction
leaked CO_2 and minerals is

$$CO_2 + H_2O = H_2CO_3$$

$$CaCO_3 + H_2CO_3 = Ca^{2+} + 2HCO_3^-$$